APR 10 '62

108328

PAPER NUMBER 61-LUBS-6

DTIC
ELECTE
SEP 2 6 1994
S F D

Non-Rotating Journal Bearings Under Sinusoidal Loads

R. M. PHELAN

Associate Professor of
Mechanical Engineering,
Sibley School of Mechanical
Engineering, Cornell University,
Ithaca, N. Y., Mem. ASME.

94-29241

The results of experimental investigations of the operational characteristics of journal bearings when carrying a sinusoidal load with zero angular velocity for both the journal and bearing are presented and compared with predictions of existing theories. Deficiencies of the analytical solutions are noted, particularly with respect to the effects of the assumed extent of the oil film, the adequacy of oil supply, the clearance ratio, and the assumed leakage path. The elementary model of approaching flat plates is discussed and the Stefan equation is modified by an area factor k, which relates equivalent circular plates to the projected area of the actual bearing. The value of k is determined from experimental data and, although the flat-plate model is found to be inadequate, the area-factor concept is shown to permit a reasonable prediction of the behavior for bearings with other than extremely small clearance. A comparison is made of the relative capacities of the squeeze and wedge films and the possibility of predicting the behavior of a statically loaded ordinary journal bearing when subjected to an additional suddenly applied load is discussed.

LIBRARY COPY
MAY 16 1961
[redacted]

Contributed by the Lubrication Division for presentation at the Lubrication Symposium, Miami, Fla., May 8-9, 1961, of The American Society of Mechanical Engineers. Manuscript received at ASME Headquarters, December 20, 1960.

Written discussion on this paper will be accepted up to June 12, 1961.

Copies will be available until March 1, 1962.

Non-Rotating Journal Bearings Under Sinusoidal Loads

108358

R. M. PHELAN

NOMENCLATURE

[illegible] = film thickness, [illegible] closest approach [illegible] journal, in.

K = area ratio, ratio [illegible] area [illegible] unit [illegible]

t = time, [illegible]

ε = eccentricity ratio, ratio [illegible] between [illegible] journal [illegible] to radial clearance

[illegible]

[illegible]

[illegible] radial [illegible]

[illegible] radial [illegible] journal, in.

D = diameter of bearing, in.

L = length of bearing, in.

N = frequency of rotation [illegible] oscillation, rps or [illegible]

N_L = load number, $\frac{[illegible]}{\mu N} \left(\frac{[illegible]}{[illegible]}\right) \left(\frac{[illegible]}{[illegible]}\right)$ [illegible]

$\frac{[illegible] P_o}{\mu N} \left(\frac{[illegible]}{R}\right) \left(\frac{[illegible]}{[illegible]}\right)$

P = unit load, psi

P_o = unit load amplitude for sinusoidal load, psi

q_m = flow rate, lb/min

R = radius of bearing, in.

R_e = radius of equivalent [illegible] flat plate, in.

S = Sommerfeld number, $\frac{\mu N}{P} \left(\frac{R}{[illegible]}\right)$

S_o = dynamic Sommerfeld number, $\frac{[illegible]}{P} \left(\frac{R}{[illegible]}\right)$

W = load, lb

INTRODUCTION

In recent years considerable attention has been given to the subject of dynamically-loaded journal bearings. Burwell ([illegible]),[1] in reporting and extending the earlier works of Harrison ([illegible]) and Swift ([illegible]), gives the most complete picture of the general case from the analytical viewpoint.

[illegible] ([illegible]) [illegible] rotation of the [illegible] [illegible] [illegible] approaching [illegible] load [illegible] [illegible] a [illegible] [illegible] carrying a [illegible] load.

[illegible] ([illegible]) [illegible] experimental [illegible] [illegible] experimental data [illegible] with theory, [illegible] [illegible] [illegible] load.

Simons ([illegible]) reported on experimental investigations carried out for a number of combinations of rotating loads and varying unidirectional loads. A [illegible] major reason appeared to be misalignment difficulties. Subsequent tests, made with the same apparatus used by Simons ([illegible]), are reported by Dayton and Simons ([illegible]) and Dayton, Simons, and Fenn ([illegible]).

Shawki ([illegible]) presented both analytical studies and experimental results for journal bearings carrying a variable load. His experimental work is the most extensive reported to date and is concerned with combinations of steady, fundamental, and harmonic components of load acting on a journal rotating at a constant speed.

Fuller ([illegible]) discusses the case of a non-rotating shaft and a unidirectional load acting on a [illegible] bearing with zero end leakage. In this case, the physical limitations on the circumferential extent of the oil film eliminate the [illegible] of negative oil-film pressures. As will be shown, this approach is the most realistic one presented to date.

The experimental results presented in this paper are limited to the study of the behavior when a sinusoidal load is applied to a journal bearing on a nonrotating shaft. Although this case is of little direct importance in design, the relative simplicity of both the analytical solution and experimental techniques appeared

---

[1] Underlined numbers in parentheses designate References at the end of the paper.

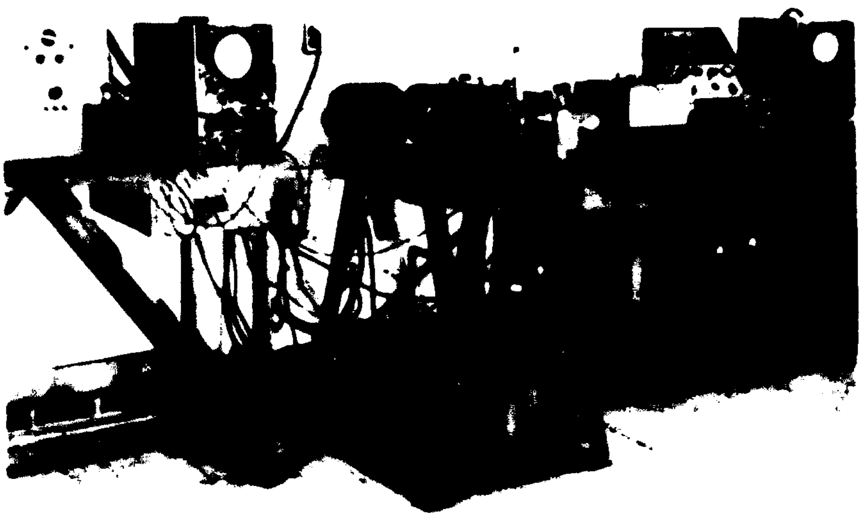

Fig. 1 Testing machine and related instrumentation

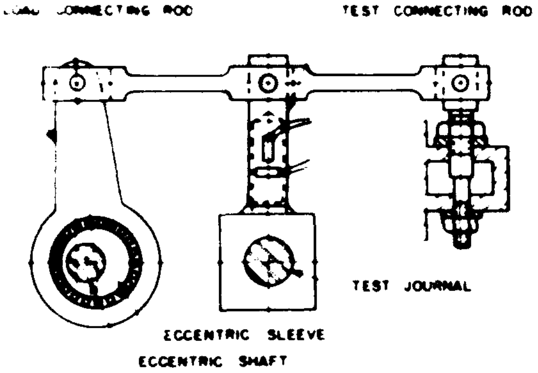

Fig. 2 Schematic drawing of method for applying a sinusoidal load on test bearing

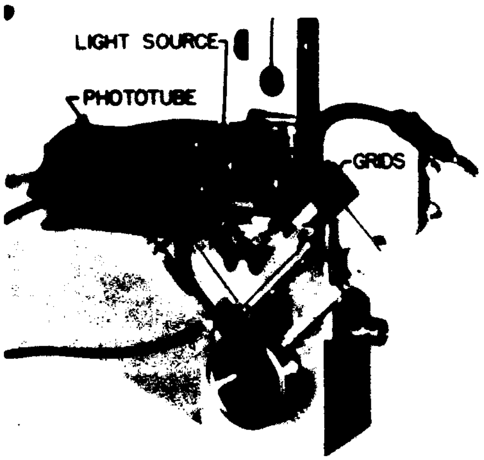

Fig. 3 Test connecting road showing photoelectric displacement pickups

to offer many advantages as a starting place in gaining a better understanding of the fundamental principles. Of particular interest is the relation of the assumptions made in reaching analytical solutions to the facts of life of bearing performance

APPARATUS

The testing machine and related equipment are shown in Fig.1. Complete details are available elsewhere (16,17) and will not be presented here. The basic elements are the loading system shown schematically in Fig.2 and the photoelectric displacement pickups shown in Fig.3. The machine is designed for applying any combination of a steady and a sinusoidal load up to maximum total load of [illegible] lb, and the shaft frequency of rotation or oscillation may be varied relative to the frequency of the loading.

The present beam dimensions are such that the maximum amplitude of the sinusoidal load component is 580 lb. A 36-tooth spline connects the eccentric sleeve to the eccentric shaft and the eccentricity can be varied in 18 steps from 0 to 0.250 in. The load is monitored continuously by use of four SR-4 type AB-7 strain gages mounted on the tubular portion of the test connecting rod, an Ellis BA-12 strain bridge, and an oscilloscope.

Each displacement pickup uses two grids having 0.01-in-wide clear spaces and opaque lines. One grid of each pickup is fixed to the connect-

A-1

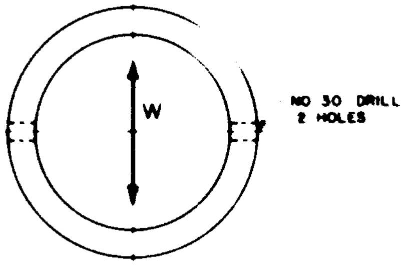

Fig. 4 Test bearing

ing rod and moves with the bearing and one is suspended by means of flex plates from the connecting rod and moves with the journal relative to the bearing. Type [illegible] bulbs and single lenses are used to provide essentially collimated light through the grids. Type 922 (vacuum) photo-tubes are used and the over-all response is linear for about 0.0043 in. of travel.

Achieving repeatable, reliable results was not a simple matter. The problem of misalignment that plagued Simons was also critical here. It is extremely difficult to maintain precise concentricity of the bearing and journal at all times while pushing and pulling on an oil film. In fact, 3 years of development, with the assistance of Messrs. J.B. Ehret, R.W. Whitlock, and J.W. Brunner, who, as undergraduate students in Mechanical Engineering at Cornell University, worked on the development and preliminary testing in connection with their fifth-year projects, were required before the author could place any confidence in the results. In this matter, the practical necessity for having the grids located axially away from the edge of the bearing turned out to be most fortunate because any angular misalignment is magnified at the grids and results in an easily recognized distortion of the trace. Unavoidable errors in manufacturing result in a change in alignment whenever the load is changed, and this is the major problem in the use of the machine. The judicious use of shims must be relied upon to correct the alignment after each adjustment. Since the measurements made are often in the order of 5 microin., there isn't much hope of eliminating this problem by making new parts.

The output from one pickup is fed to the Y-axis input and the other to the X-axis input of an oscilloscope, where they combine to produce a dot that traces out the path of the journal in the clearance circle. The cathode-ray tube has been rotated 45 deg so that the orientation of the trace on the oscilloscope screen corresponds directly to the actual case.

In use, no attempt is made to calibrate the pickups in terms of inches of travel; but since the sinusoidal load is applied vertically and the pickups measure the 45-deg components of the vertical motion, it is a simple matter to adjust the sensitivities of the pickups so that when operating at low frequencies with no oil the travel from top to bottom of the clearance space is 2.00 inches on the screen. Thus, the clearance circle is defined as a circle with a one-inch radius and the eccentricity ratio ϵ and attitude angle ϕ may be read directly.

The nominal dimensions of the bearing are L = D = 1.25 in. The ratio L/D = 1 was chosen so that both infinite and short bearings may be compared in terms of the same dimensionless numbers. Here the term infinite bearing applies to the case in which end leakage is neglected ([illegible]), and the term short bearing applies to the case in which end leakage is included and circumferential flow due to pressure is neglected (3). Since the bearing must be finish-bored after being pressed into the connecting rod, different clearance ratios are achieved by using test shafts with different diameter journals.

EXPERIMENTAL RESULTS

The early tests were carried out with the bearing shown in Fig.4. Oil inlet through two holes on the horizontal plane was chosen to prevent loss of load-carrying capacity due to a decrease in film pressure in the vicinity of the inlet holes. Smith (17) carried out extensive investigations with three clearance ratios, 0.00088, 0.00160, and 0.00288 in./in.; frequencies from 100 to 845 cpm; nominal load amplitudes from 101 to 333 lb (corresponding to bearing pressures of 65 to 213 psi on projected area); and with oil supply pressures ranging from 27.5 to 150 psi. No attempt was made to control the oil temperature and the viscosity of the standard SAE 10 motor oil varied between 2.7 and 9 microreyns.

Although the presentation of Smith's thesis is not the purpose of this paper, his results were instrumental in dictating the path of the investigations that are of immediate interest and some of them will be discussed here. Smith followed the notation of Shaw and Macks (18) and used the dynamic Sommerfeld number

$$S_o = \frac{\mu\,\omega}{P_o}\left(\frac{R}{C}\right)^2$$

as the independent variable and the eccentricity ratio as the dependent variable. However, using either this or the more common form

$$S = \frac{\mu N}{P}\left(\frac{R}{C}\right)^2$$

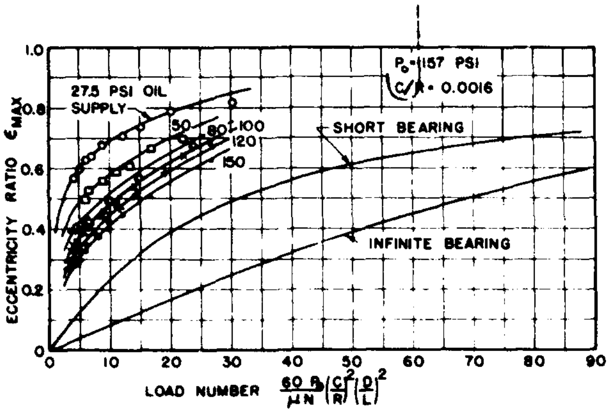

Fig. 5 Variation of the maximum eccentricity ratio with oil-supply pressure and load number

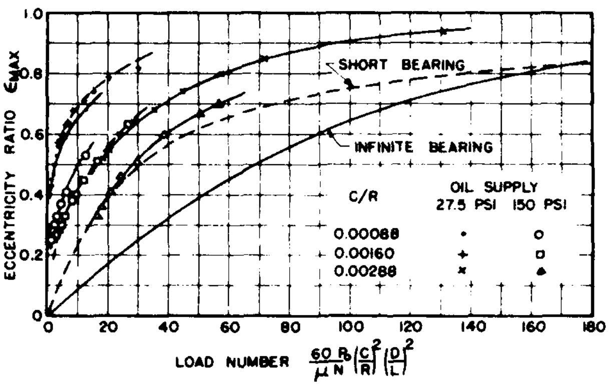

Fig. 6 Variation of the maximum eccentricity ratio with clearance ratio, oil-supply pressure, and load number

compresses the data in the region of high eccentricity ratios, which is the region of most importance to the designer. To avoid this difficulty and to simplify extending the discussion to include short bearings as well, a new dimensionless number, called the load number by Ocvirk (12), will be used in this paper. The load number is defined as

$$N_L = \frac{60P}{\mu N}\left(\frac{C}{R}\right)^2\left(\frac{D}{L}\right)^2 \text{ or } \frac{60P_o}{\mu N}\left(\frac{C}{R}\right)^2\left(\frac{D}{L}\right)^2$$

where P_o is the sinusoidal load amplitude, and, except for the $(D/L)^2$ term, it is the inverse of the Sommerfeld number.

Fig.5 is based on Smith's data for a series of tests made with a clearance ratio of 0.00160 in./in. and a load amplitude of 157 psi. The obvious conclusion is that neither the long-bearing nor the short-bearing approximation is adequate. The major deviations are that the actual bearing operates with a considerably thinner minimum oil film and the oil-supply pressure is a major factor, although neglected by both theories.

Fig.6 is also based on Smith's data and illustrates the effect of clearance ratio on performance. The most significant observation here is that, at least for the clearance ratios used, neither approximation adequately accounts for the effect of clearance ratio. It should also be noted that the greater the clearance, the thicker the oil film, and that the curve for the 0.00288 clearance ratio with 150 psi oil-supply pressure corresponds closely to that of the short-bearing approximation. Also, it should be noted that the results for the small and medium clearance cases lie fairly close together while the results for the large clearance case lie off by themselves.

The deviations from the theoretical curves appear to be due to the inadequacy of three assumptions: (a) That the clearance space is at all times completely filled with oil, (b) that the negative pressures contribute fully to supporting the load, and (c) that the oil flow due to pressure in the film is in either the circumferential or axial direction, but not in both.

Failing to fill completely the clearance space on the unloaded side of the bearing during the short time available is the main reason for finding a family of curves based on oil-supply pressure in Fig.5 and a family of curves based on clearance ratio in Fig.6. As shown in Fig.4, the oil is introduced at the sides. Equilibrium is reached when the oil supplied balances the oil lost due to flow in the axial direction.

Fig.7 shows Smith's data for oil flow as affected by clearance, oil-supply pressure, and load. The actual flow rates have been adjusted by multiplying by the ratio of the actual viscosity to the viscosity at 80 F to minimize the effect of viscosity on flow rate. The data are meager but it seems apparent that the clearance and oil-supply pressure are the major factors and the load magnitude is relatively unimportant. Smith also shows that the oil flow rate is practically independent of the load frequency. These results are consistent with the observations related to variation of eccentricity with clearance and with oil-supply pressure. For the smaller clearances, with very little oil flow, even the maximum pressure does not provide sufficient flow from the two holes to maintain a complete (2π) oil film. When the clearance is increased, the oil flow due to the supply pressure is increased and it is more nearly possible to keep the clearance space filled with oil at all times.

Recently a series of investigations has been made with a modified bearing to provide (a) more insight into the problem of oil supply, (b) performance data for operation at higher load numbers, (c) data for determining the reasonability of the assumption of a 2π film, and the resulting

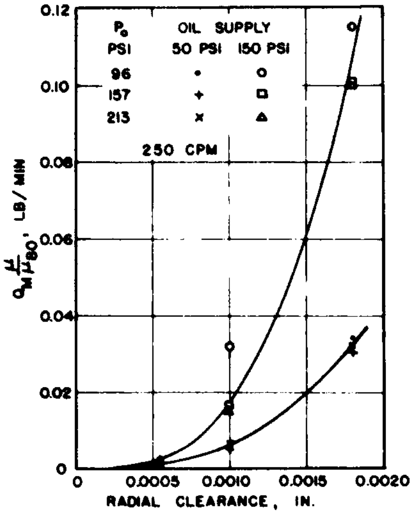

Fig. 7 Variation of oil-flow rate with oil-supply pressure and radial clearance

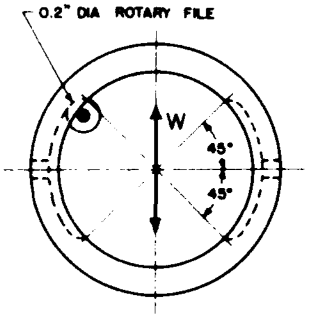

Fig. 8 Modified test bearing

contribution to capacity of high negative pressures in the oil film, and (d) data for determining whether or not it would be possible to correlate the experimental results with a mathematical model based on the Stefan equation for approaching flat plates.

Oil grooves were cut into the bearing, by use of a spherical rotary file as shown in Fig.8, to increase the flow of oil into the unloaded side of the bearing. This increased flow is at the expense of a loss in load-supporting area, due to the grooves extending down into the region in which the squeezing action develops pressure in the oil film.

During the interval between Smith's tests and those to be discussed, the Sibley School of Mechanical Engineering moved into a new building and one of the few items lost during the moving operation was a parts box containing two shafts for this machine. Consequently new shafts had to be made. The resulting clearance ratios are now 0.00075, 0.00195, and 0.00288 in./in., with

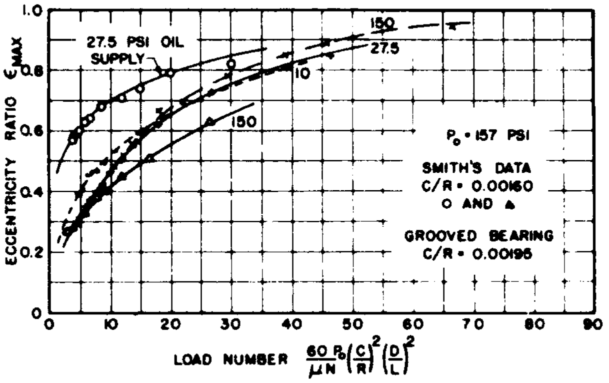

Fig. 9 Comparison of results for the modified (grooved) bearing with those for original bearing

the latter being the same for both series of tests.

Another variation in test conditions is that Smith used an SAE 10 W oil with a viscosity of 4.27 microreyns at 100 F whereas the oil used in the current tests has a viscosity of 5.46 microreyns at 100 F.

Theoretically both the clearance-ratio and viscosity variations should be accounted for by the load number, but since Smith's results point out the inadequacy of the load number in these respects, they cannot be ignored when making direct comparisons of results.

The effect of adding the oil grooves is graphically shown in Fig.9 for the medium clearance case. The most striking observation is that the effect of oil pressure is much less with the grooves than with the holes only. Even a supply pressure as low as 10 psi (a condition for which Smith presents no results) gives results comparable to those with 150 psi supply. It should also be noted that in comparison with Smith's data the oil groove results in appreciably lower values of ϵ_{max} when the oil supply pressure is low and in appreciably higher values of ϵ_{max} when the oil supply pressure is high. Apparently at low pressures the grooves' assistance in filling up the space on the unloaded side more than compensates for the loss in area, while with a high (150 psi) pressure supply, the holes provide a more nearly adequate oil supply and the loss of area becomes significant.

A comparison of the curves for the oil-groove runs shows that lower pressures give greater values of ϵ_{max} at low values of N_L while the reverse is true at high values of N_L. Low values of N_L correspond here to high frequencies of load variation and the time interval seems to be too short for the low-pressure oil supply to fill completely the unloaded side of the bearing. High values

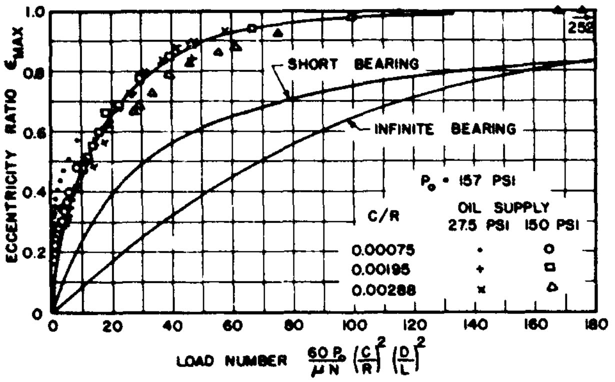

Fig. 10 Variation of maximum eccentricity ratio with oil-supply pressure, clearance ratio, and load number for the grooved bearing

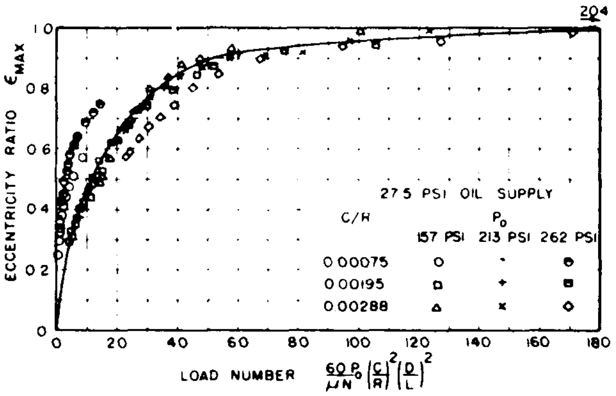

Fig. 11 Variation of the maximum eccentricity ratio with clearance ratio, load amplitude, and load number for the grooved bearing

of N_L correspond here to low frequencies of load variation and one would expect the curves to be closer together — with possibly slightly greater values of ϵ_{max} with the lower pressure oil supply. Actually, the reverse is true and ϵ_{max} is greater for the high pressure supply. This will be again referred to below but, for the present, it is sufficient to say that it is felt that the explanation lies in the fact that since there is no positive control of the oil temperature, the temperature of the oil supplied to the bearing is closely related to the pressure and clearance. In these tests the viscosities at the higher values of N_L were 4.4, 7.9, and 8.0 microreyns for the 150, 27.5 and 10 psi cases, respectively. Again, this may be interpreted as evidence pointing to the inadequacy of existing theory.

Fig.10 is a plot of results for runs made with 27.5 and 150 psi oil-supply pressure for the three clearance ratios. In comparing these curves with those based on Smith's data, Fig.6, for operation under comparable conditions a number of differences are immediately apparent: (a) The large-clearance curves with high-pressure oil supply now deviate much more from the short-bearing prediction than before the grooves were added, (b) all points lie much more closely together, (c) the medium-clearance points now agree more closely with those for the large-clearance case, and (d) values of $\epsilon_{max} = 1.0$ were noted at the highest load numbers.

Observations (a), (b), and (c) are all related to the effect of the oil-groove on the oil supply and on the loss in load supporting area.

The explanation for the shift in agreement between the results for the small and medium clearances with the oil holes only to agreement between the results for the medium and large clearances with the oil grooves lies again in the relationship of clearance to oil supply. Smith's tests were made with clearance ratios of 0.00066, 0.00160 and 0.00288 in./in. while the grooved-bearing tests were made with ratios of 0.00075, 0.00195 and 0.00288 in./in. In Smith's case, the oil pressure has been shown to have the greatest significance. Combining this with a larger value for the small clearance and a smaller value for the medium clearance, one might expect that a low pressures the supply of oil to the unloaded side of the bearing would be quite small for both the small and the medium clearances, while at high pressures, the medium clearance bearing would receive a more nearly adequate supply and would therefore perform better. The curves in Fig.6 are in complete agreement with both hypotheses.

When the grooves are added, the oil supplied to the unloaded side of the bearing is almost equalized for all clearances and pressures. The major deviation is for the small clearance ratio of 0.00075 in./in., but, even here, the deviation from the results for the large clearance case is much less than for operation with holes only and a somewhat larger clearance ratio of 0.00088 in./in. The difficulty of supplying sufficient oil with the very small clearance is further emphasized by noting in Fig.10 that the eccentricity ratio curve for the 150 psi oil supply falls appreciably below that for the 27.5 psi oil supply.

The great difference in behavior with very small clearances is readily noted in a qualitative manner by operating with some oil supply pressure until equilibrium is reached and then shutting off the oil and observing what happens. For the large-clearance case, the maximum eccentricity ratio increases to 1.0 in a few seconds, as evidenced both by observance of the trace on the oscilloscope screen and by a loud, sharp knocking sound. The medium-clearance case re-

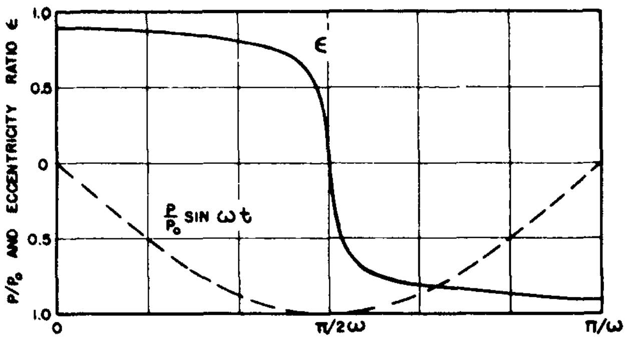

Fig. 12 Variation of eccentricity ratio with time as predicted by Burwell (3) for a sinusoidal load

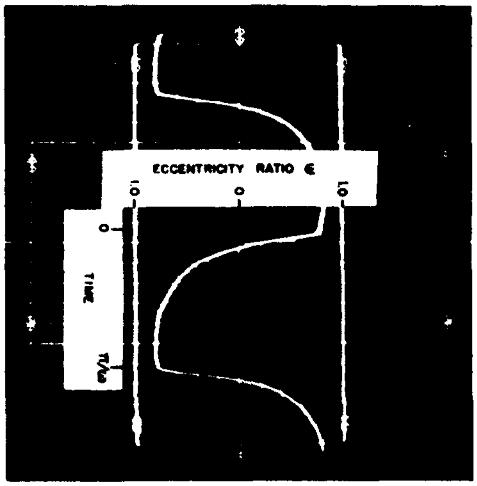

Fig. 13 Experimentally determined variation of eccentricity ratio with time for a sinusoidal load

quires several more seconds but metal-to-metal contact is still made in a very short time. For the very small clearance, the eccentricity ratio increases much more slowly and will still not have reached 1.0 at the end of 30 min. The eccentricity ratio will increase somewhat faster, but only to a slightly larger value, on the top side. Apparently, the clearance is so small that capillary action keeps the oil not only from being squeezed out and lost but from even running down under the force of gravity.

In terms of fundamental behavior, observation (d) is particularly important. In more detail, $\epsilon_{max} = 1.0$ was noted at the two highest values of N_L and this value was approached far more rapidly than either theory predicts. Because of the inherent problems of misalignment, calibration of the oscilloscope pattern, and reading the deflection on the oscilloscope screen, it is rather difficult to prove that the journal actually contacted the bearing surface through a breakdown of the oil film. However, a distinct knock could be felt when placing one's hand on the top of the connecting rod.

Fig.11 compares results for tests made with three load amplitudes; 157, 213 and 262 psi. Since practical bearings operate with relatively low oil-supply pressures and since the effect of oil pressure on the bearing with oil grooves is not great, the only data considered here are for 27.5-psi supply. Again, as in Fig.10, there is some scatter of points for the medium and large clearance-ratio cases. However, if the points for the 262-psi load amplitude and large clearance are ignored, the remaining five sets of points plot as one curve while the points for the small-clearance case lie close together but at a considerable distance from the other curve.

OBSERVATIONS RELATED SPECIFICALLY TO THE THEORY

Aside from the very practical and important consideration of filling the space on the unloaded side of the bearing with oil, the major possible sources of difference between the predictions of the theories available at this time and the observed behavior are (a) the assumption of a complete (2π) oil film and (b) the assumption of a bearing with either infinite or zero length.

There is general agreement that oil films in journal bearings cannot carry a tensile stress and cavitation exists in regions where the absolute pressure is less than the vapor pressure of the lubricant. Thus, in practice, cavitation is to be expected in all but very lightly loaded bearings (21, 22).

Fig.12 shows the relationship between ϵ and P as functions of time according to Burwell's (3) development of the short bearing approximation. Fig.13 is a photograph of ϵ as actually observed, including the effects of deflection. The difference arises because theories based on a 2π film, and thus support by negative pressure, result in curves for ϵ that possess a type of symmetry about the peak load, or $\omega t = \pi/2$, whereas in reality the negative-pressure support is negligible and the entire curve looks something like the last half of the theoretical curve.

On the basis of these figures it seems obvious that there is little point in pursuing much further analytical studies based on a 2π oil film.

At the same time, the knowledge that only the positive pressures materially contribute to supporting a load led directly to the analogy between the journal and bearing and Stefan's (7) solution for approaching elliptical flat plates. The analogy could not be expected to be perfect because (a) the projected area or even the developed area for a bearing is in general a rectangle, not an ellipse, and (b) the film thickness between the journal and the bearing is not uniform over the entire area. The shape of the area was not felt to be too critical because it should be possible to work with an equivalent ellipse, with the constant of proportionality determined empirically. The importance of the variation in film thickness was actually given relatively little thought until later but it seemed logical that again an empirically determined constant would allow for its effect. At the same time the use of an equivalent area based on experimental results would take into account the actual pattern of oil flow from the finite length bearing.

FLAT-PLATE ANALOGY

The usefulness of this analogy lies in the relative ease with which the film thickness can be calculated for any type of loading. Assuming the projected area of the bearing to be the logical basis for comparison, the solution for approaching flat rectangular plates would appear to be most desirable. Since the solution for this case does not exist it becomes necessary to consider the next closest approximation for which a solution exists, approaching ellipses.

At first glance, ellipses appear to be a reasonable approximation in that one axis can be made proportional to the bearing diameter and the other to the bearing length. The difficulty inherent in this approach is that if the total area is kept constant, the behavior predicted would be the same for a bearing with L/D = 1/2 as for a bearing with L/D = 2. Experience has shown that end leakage decreases the load capacity when carrying a static load with a rotating journal and it did not seem likely that the behavior of a squeeze-film bearing would be independent of the value of L/D. The actual significance of L/D will be discussed later but for the time being only the ratio L/D = 1, corresponding to the test bearing, need be considered. In this case the equivalent flat plates become circles and the rate of change of film thickness with time may be shown to be

$$\frac{dh}{dt} = \frac{2Wh^3}{3\mu\pi R_e^4} \qquad (1)$$

where R_e is the radius of the equivalent circle and W is the load. W will be a negative number because its direction is opposite to that of positive h.

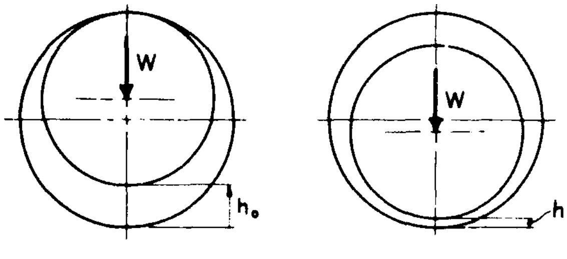

(a) $t = t_o$ (b) $t_1 = t_o + \Delta t$

Fig. 14 Film thickness definition

The relationship of the area of the equivalent circle to the projected area of the bearing with L = D is

$$\pi R_e^2 = kLD = 4kR^2 \qquad (2)$$

from which

$$R_e = 2\left(\frac{k}{\pi}\right)^{1/2} R \qquad (3)$$

Substituting for R_e in equation (1), gives

$$\frac{dh}{dt} = \frac{\pi W h^3}{24\mu k^2 R^4} \qquad (4)$$

In terms of the unit loading $P = W/4R^2$ equation (4) becomes

$$\frac{dh}{dt} = \frac{\pi P h^3}{6\mu k^2 R^2} \qquad (5)$$

For the particular bearing used here R = 0.625 in. and equation (5) becomes

$$\frac{dh}{dt} = \frac{1.34\, P h^3}{\mu k^2} \qquad (6)$$

Assuming, as a first approximation, that k is a constant, separating the variables gives

$$\frac{1}{h^3}\, dh = \frac{1.34}{\mu k^2}\, P\, dt \qquad (7)$$

which upon integration and rearranging becomes

$$\frac{1}{h^2} = -\frac{2.68}{\mu k^2}\int P\, dt + K \qquad (8)$$

For a journal bearing, h will be the thickness of the oil film measured at the point of closest approach of the journal to the bearing and new initial conditions must be used each time the load reverses direction. For example, in Fig.14 the journal position is shown at time t_o in (a) and a short time later in (b).

For steady-state operation with a sinusoidal load when $h = h_o$ at $t = 0$ and $P = -P_o \sin \omega t$,

$$\frac{1}{h^2} = \frac{-2.68P_o}{\mu k^2 \omega}\cos \omega t + \frac{2.68P_o}{\mu k^2 \omega} + \frac{1}{h_o^2} \qquad (9)$$

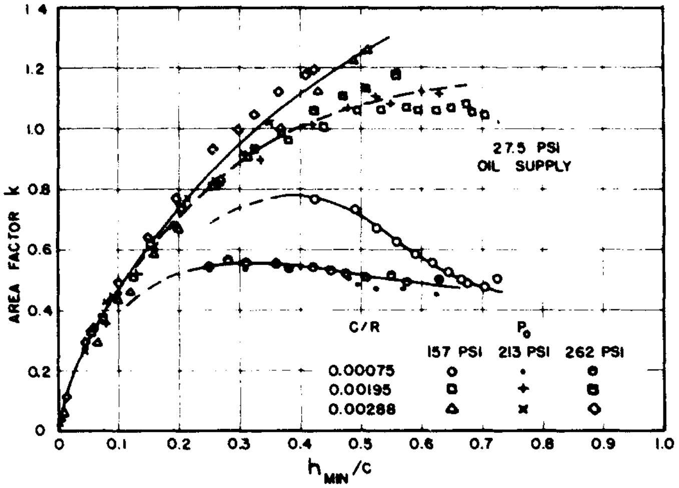

Fig. 15 Variation of area factor with clearance ratio, load amplitude, and ratio of minimum film thickness to radial clearance. Area factor assumed constant during each test

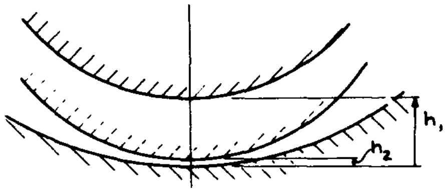

Fig. 16

The minimum film thickness h_{min} occurs when ωt = 180 deg and

$$\frac{1}{h_{min}^{2}} = \frac{5.36P_o}{\mu k^2 \omega} + \frac{1}{h_o^{2}} \qquad (10)$$

Solving equation (10) for k gives

$$k = \left[\frac{5.36\,P_o}{\mu\,\omega\,\left(\frac{1}{h_{min}^{2}} - \frac{1}{h_o^{2}}\right)}\right]^{1/2} \qquad (11)$$

where, in terms of experimental measurements

$$h_o = C\,(1 + \epsilon_{max}) \qquad (12)$$

and

$$h_{min} = C\,(1 - \epsilon_{max}) \qquad (13)$$

Values of k^2 and k were calculated for the grooved bearing with 27.5 psi oil-supply pressure and for the three clearance ratios of 0.00075, 0.00195 and 0.00288 in./in. and the three loads of 157, 213 and 262 psi, the data being the same as used in plotting Fig.11. Although k^2 is the more important from the load-capacity viewpoint, k, which is a measure of how effective the actual bearing is relative to the flat plates, offers more insight into fundamental behavior and will be considered here.

Values of k are shown in Fig.15 as functions of h_{min}/C or $1 - \epsilon_{max}$. The observations of most interest are that (a) k is not a constant but varies with film thickness and clearance, (b) all curves reach zero at zero film thickness, and (c) values of k were found to exceed 1.0.

As pointed out previously, the effect of clearance is most apparent for the very small clearance case. However, in general, smaller clearances result in a decrease in relative effectiveness, particularly for thicker films. The reason seems, again, to be simply that the greater film thicknesses are developed at higher load frequencies and with small clearances the resistance to oil flow is so great that the unloaded side cannot be filled in the short time available. From a practical viewpoint, this is not critical. The agreement between the medium and large clearance curves is good in the region where operation may be critical; i.e., $\epsilon > 0.7$, or $h_{min}/C < 0.3$.

Although the small clearance appears to be rather inefficient in terms of k, it should be noted that even under the most extreme test conditions (a load magnitude of 262 psi and a load frequency of only 105 cpm) ϵ never exceeded 0.75. Since the experimental curves indicate that k is not a constant but is a function of h/C, the values plotted are significant only for sinusoidal loads and represent some sort of an average over the total displacement.

The major reason for k, and thus k^2, approaching zero as h approaches zero lies in the geometry of the cylindrical surfaces. For example, as shown in Fig.16, the film thickness is more nearly uniform when the journal is relatively far away from the bearing at h_1 than it is at h_2 when there is almost metal-to-metal contact. Thus, although the total capacity may not be as great, h_1 is a better approximation to an effective film thickness than is h_2, which would be appropriate only over a small region near the point of closest approach.

If the effective area is to have any practical value to the designer, a better estimation of the relationship of k^2 to h/C is necessary. Letting $k^2 = f(h/C)$, equation (6) may be rewritten as

$$\frac{f(h/C)}{h^3}\,dh = \frac{1.34}{\mu}\,P\,dt \qquad (14)$$

or

$$f(h/C) = \frac{1.34\,P\,h^3}{\mu\,dh/dt} \qquad (15)$$

The straightforward approach is to substitute experimentally determined values for h^3 and dh/dt and known values of P into equation (15) and solve for $f(h/C) = k^2$.

This sounds relatively simple and attempts have been made and are continuing to be made to arrive at satisfactory results, but the problems become rather formidable in terms of compensating for shaft deflections, graphically differentiating for dh/dt, and above all accurately measuring h in the important region where h $<$ 100 microinches.

Another approach is to apply curve fitting by assuming a form for $k^2 = f(h/C)$ and solving for the constants by using the sinusoidal test data. Here the first step was to plot the values of k^2 for the medium and large clearance points. The resulting curve had no direct significance in itself but it indicated that, although there might not be a simple expression that would cover the entire range from $0 \leq h/C \leq 2.0$, a curve of the form

$$k^2 = A\left(\frac{h}{C}\right)^a \qquad (16)$$

would be a reasonable approximation, at least in the region where $h/C < 0.4$. Since the load capacity of the squeeze film is appreciable only for very thin films, it was felt that the error introduced at large values of h/C might be negligible and far outweighed by the convenience of being able to solve equation (14) directly for h for any type of loading; e.g., square-wave, steady plus sinusoidal, and so on.

Substituting equation (16) in equation (14) and simplifying gives

$$h^{a-3}dh = \frac{1.34\ C^a}{A\mu}\ P\ dt \qquad (17)$$

Integrating equation (17) for $P = -\ P_o \sin \omega t$, substituting limits, and rearranging gives

$$\frac{1}{h_{min}^{-(a-2)}} - \frac{1}{h_o^{-(a-2)}} = -\ \frac{2.68\ (a-2)\ C^a}{A\ \mu\ \omega}\ P_o \qquad (18)$$

Then, data corresponding to two points on the curve of k^2 versus h/C were selected and equation (18) was solved for a and A. The resulting expression for k^2 is

$$k^2 = 2.46\ \left(\frac{h}{C}\right)^{1.72} \qquad (19)$$

and equations (17) and (18) becomes, respectively

$$h^{-1.28}dh = \frac{0.545\ C^{1.72}\ P\ dt}{\mu} \qquad (20)$$

and

$$\frac{1}{h_{min}^{.28}} - \frac{1}{h_o^{.28}} = \frac{0.305\ C^{1.72}\ P_o}{\mu\ \omega} \qquad (21)$$

Upon substituting equations (12) and (13) for h_o and h_{min}, making other substitutions, and rearranging terms, equation (21) becomes simply

$$\frac{1}{(1 - \epsilon_{max})^{.28}} - \frac{1}{(1 + \epsilon_{max})^{.28}} = \frac{N_L}{52.7} \qquad (22)$$

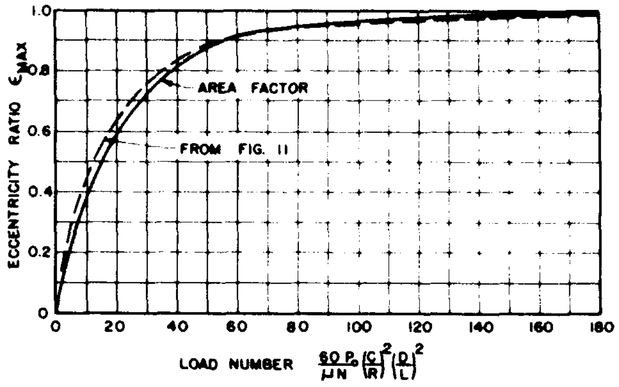

Fig. 17 Comparison of area-factor prediction with experimental results

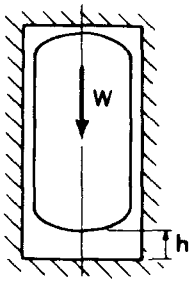

Fig. 18 Model for squeeze-film lubrication with zero rotation of load, shaft, and journal

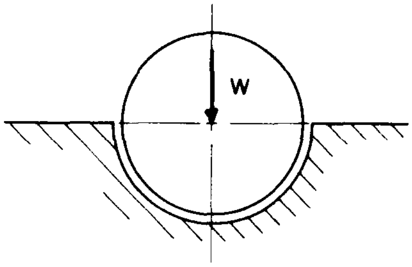

Fig. 19 Bearing treated by Fuller (15)

The curve for the relationship in equation (22) is given in Fig.17 where it may be compared with the experimental curve reproduced from Fig. 11. The agreement between the curves is in general quite good. In fact, if the equation (22) curve is drawn in Fig.11, it will be found to lie within the scatter of points, except for low eccentricity ratios.

The maximum value of k from equation (19) is 2.85, which at first seems to be ridiculous. Undoubtedly, k is somewhat too high for larger values of h/C. This is indicated by the prediction of lower eccentricity ratios at low values of N_L than actually observed. However, even here the

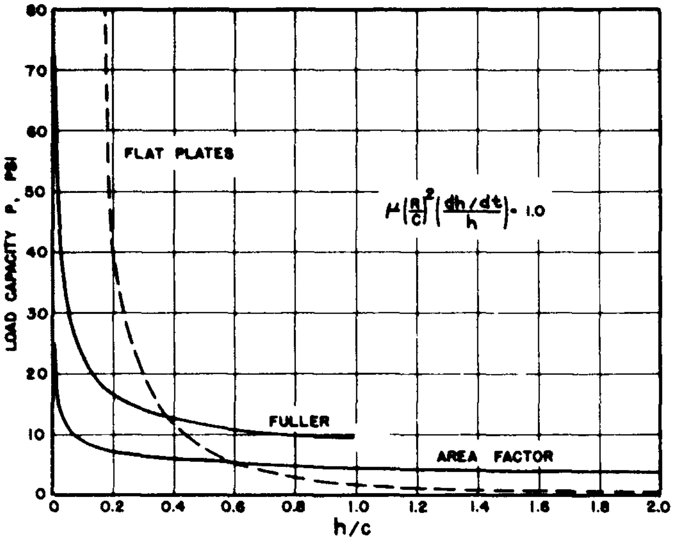

Fig. 20 Comparison of load capacities predicted by the area-factor equations, Fuller's (15) equation, and flat-plate equation

difference is not great and, therefore, it seems reasonable that the error in k is also not great. Again, from a purely practical viewpoint, this becomes inconsequential because low values of N_L correspond to low values of ϵ_{max} where operation is not critical.

However, the really significant conclusion based on the variation of k with h/C is that the model of approaching flat plates is not the proper one to use in the first place, for two important reasons; (a) The effect of curvature on the effective value of h as discussed previously, and (b) the fact that the bearing clearance space is a closed system if end leakage is neglected and almost closed even if end leakage is considered. A more appropriate model is the loose fitting piston with curved ends in a cylinder shown in Fig.18. Downward motion of the piston results in the development of a pressure because of the ordinary squeeze effect previously considered and because of the pumping losses in moving the oil from underneath to above the piston. For this model, the pumping losses are independent of h and the squeeze effect becomes appreciable only when h becomes very small. It is apparently a very fortunate coincidence that the empirical relationship for k adequately expresses both effects. Further evidence of the validity of the above conclusion is given by a comparison of Fuller's (15) solution for the half-bearing with the experimental curves. Fuller considers the case in Fig.19. Here the eccentricity ratio can vary only from 0 to 1.0 and end leakage is considered to be zero. His expression for the instantaneous load capacity is

$$W = \frac{\mu\ L\ dh/dt}{(C/R)^3}\ [K] \qquad (23)$$

$$\text{where } K = f(\epsilon) = 12\left[\frac{2}{(1-\epsilon^2)^{2/3}}\tan^{-1}\frac{(1-\epsilon^2)}{1-\epsilon}^{1/2} + \frac{\epsilon}{1-\epsilon^2}\right]$$

A comparison could be made on the basis of assuming a constant value of dh/dt for both cases and calculating W as functions of ϵ only. However, it is also a matter of considerable interest to compare the capacity of the squeeze film with that of the wedge film of an ordinary journal bearing carrying a static load. For this purpose the assumption of a constant velocity of approach is too unrealistic, simply because the physical limitations require dh/dt → 0 as h → 0. Although no absolute comparison can be made, a fairly realistic basis for a relative comparison will be to let the velocity vary directly with film thickness; i.e., (dh/dt)/h = constant.

Rewriting equation (23) in terms of P and (dh/dt)/h gives for Fuller's case

$$P = \frac{\mu}{2}\left(\frac{R}{C}\right)^2\left(\frac{h}{C}\right)\left(\frac{dh/dt}{h}\right)[K] \qquad (24)$$

Similarly, rewriting equation (5) in terms of $k^2 = 2.46\ (h/C)^{1.72}$ and solving for P gives for the area-factor case

$$P = 4.69\ \mu\left(\frac{R}{C}\right)^2\left(\frac{h}{C}\right)^{-.28}\left(\frac{dh/dt}{h}\right) \qquad (25)$$

Letting

$$\mu\left(\frac{R}{C}\right)^2\left(\frac{dh/dt}{h}\right) = 1\text{ psi} \qquad (26)$$

equation (24) becomes

$$P = \frac{1}{2}\left(\frac{h}{C}\right)[K]\text{psi} \qquad (27)$$

and equation (25) becomes

$$P = 4.69\left(\frac{h}{C}\right)^{-.28}\text{psi} \qquad (28)$$

Curves calculated by use of equations (27) and (28) are shown in Fig.20. The main observations are that both curves have the same general form and that the area factor curve indicates less load carrying ability than does Fuller's solution.

Although Fuller's solution, in its present form, cannot be extended to values of h/C > 1.0, the similarity of the curves is so great that it seems only reasonable to expect the extension to continue in much the same manner as does the area-factor curve.

The lower capacity shown by the area-factor curve is to be expected because it is based on experimental results and includes the leakage effects due to the finite length and the oil grooves, neither of which is considered in

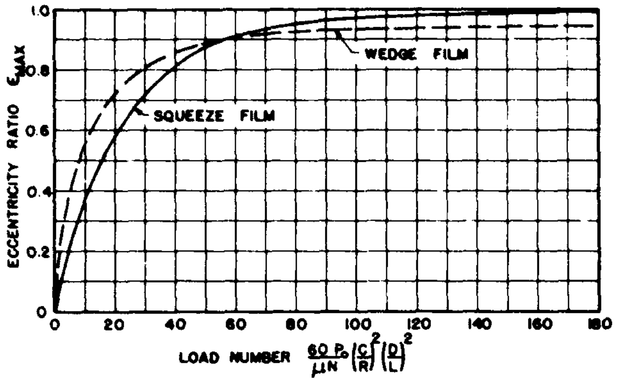

Fig. 21 Variation of maximum eccentricity ratio with load number for squeeze-film and wedge-film bearings

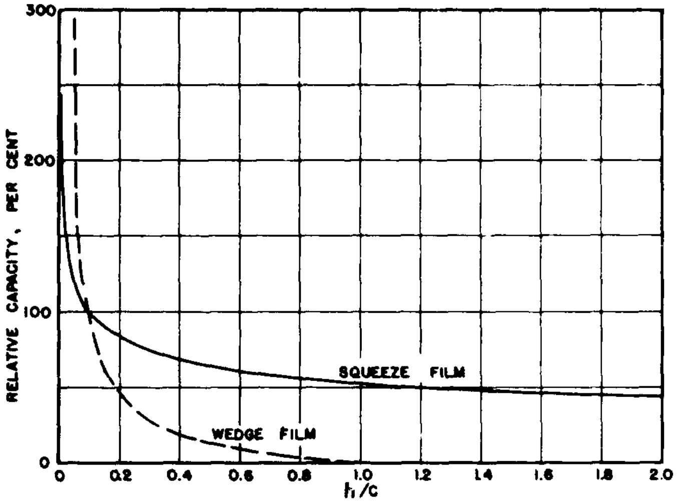

Fig. 22 Comparison of the relative capacities of the squeeze film and wedge film as functions of ratio of film thickness to radial clearance

Fuller's solution. It should also be noted that if Fuller's solution were to be interpreted in terms of the area factor, the values of k would be considerably greater than found experimentally and therefore finding values of k greater than 2.5 is not at all unreasonable.

To emphasize further the great difference between the flat-plate analogy and experimental results, a curve showing the relative capacity of two circular plates with areas equal to the projected area of the bearing has been included in Fig.20. The flat-plate curve intersects the area-factor curve at $h/C = 0.59$ where k for the area-factor case equals 1.0.

COMPARISON OF SQUEEZE-FILM AND WEDGE-FILM PERFORMANCE CHARACTERISTICS

One basis for comparing the performance of the squeeze film with that of the wedge film is to compare the value of ϵ_{max} for a sinusoidal load with zero rotation and a load frequency of N cpm with ϵ for a static load equal to the amplitude of the sinusoidal load and a journal speed of N rpm. Furthermore, since the area-factor curve is based on experimental results, the comparison will have more significance if the wedge-film curve is also based on experimental results. Fig.21 compares the wedge-film experimental results of DuBois, Ocvirk, and Wehe (20) with the area-factor curve given by equation (22). As can be seen, the squeeze-film case gives smaller eccentricities, and thus thicker films, for $\epsilon < 0.9$ and larger eccentricities for $\epsilon > 0.9$. The superiority of the wedge film for values of $\epsilon > 0.9$ is graphically shown by the wedge-film curve being almost horizontal while the squeeze-film curve is still approaching $\epsilon = 1.0$ at a rapid rate.

From the viewpoint of gaining a better understanding of the fundamental behavior characteristics, a comparison based on the instantaneous capacities of the films as functions of the journal position in the clearance space is far superior to the comparison just made on the basis of sinusoidal loading. However, even if all other parameters are held constant, the squeeze-film load capacity, equation (25), is a function of both the position of the journal and the velocity with which the journal is approaching the bearing, whereas the load capacity of the wedge film is a function of only the position. Therefore, again, it is impossible to compare the squeeze-film and wedge-film capacities in absolute terms and any relative comparison must be qualified by the assumed conditions. Here, the basis for comparison is that $(dh/dt)/h$ is a constant for the squeeze-film case and that the wedge-film capacity is equal to that of the squeeze film when $\epsilon = 0.9$, or $h/C = 0.1$. Utilizing equation (25) for the squeeze film and Fig.21 for the wedge film, the capacities relative to that at $h/C = 0.1$ have been calculated and the curves are presented in Fig.22.

In general the conclusions drawn from Fig.22 are the same as those drawn from Fig.21. However, showing the capacities as functions of the film thickness emphasizes the different characteristics of the two films. The obvious, and very important, difference is that the squeeze-film capacity is appreciable over the entire range of h/C while the wedge-film capacity becomes appreciable only when h/C is small. Noting the rapid increase in the wedge-film capacity with decreasing film thickness leads to the observation that for thin films, the wedge film is much more effective than is the squeeze film.

In a practical situation the case often arises in which a bearing carrying a static load is subjected to a sudden increase in load that acts for a relatively short time. Numerous authors have discussed this in terms of the squeeze film carrying all of the suddenly applied load. A better approach would be to consider that the instantaneous load capacity is the sum of that due to the wedge film and that due to the squeeze film. Since the squeeze film requires a velocity dh/dt in order to develop pressure, the eccentricity ratio will increase and the wedge-film capacity will also increase. The question then is - how is the load distributed between the films?

One of the major difficulties in combining the load capacity of the squeeze film with that of the wedge film is that relative motion between the journal and bearing is along a radial line for the squeeze-film case, while it follows approximately a semicircle for the wedge-film case (20). Although there is no experimental evidence confirming this, it is felt that for a heavily loaded bearing, i.e., $\epsilon > 0.9$, no serious error will be introduced by ignoring the difference in paths of travel with increasing load. The discussion below will offer a logical basis for this.

Equation (25) may be used to calculate the velocity dh/dt required, under a given set of conditions, for the squeeze film to support a specific instantaneous load. However, as a matter of convenience, it is desirable to work in terms of the rate of change of the eccentricity ratio. By definition

$$\frac{h}{C} = 1 - \epsilon \qquad (29)$$

and, therefore,

$$\frac{dh/dt}{C} = -\frac{d\epsilon}{dt} \qquad (30)$$

In terms of $d\epsilon/dt$, equation (25) may be rewritten as

$$\frac{d\epsilon}{dt} = -\frac{P}{4.69\,\mu}\left(\frac{C}{R}\right)^2\left(\frac{h}{C}\right)^{1.28} \qquad (31)$$

To illustrate a possible approach to considering both squeeze and wedge films at the same time, let us consider a bearing under the following operating conditions: P = 1000 psi, N = 1000 rpm, C/R = 0.00288 in./in., L/D = 1, and $\mu = 6.0$ microreyns. The load number is calculated to be 83 and from Fig.21 the steady-state eccentricity ratio is found to be 0.93. Assume now, although it is a physical impossibility, that the load is instantaneously increased to 2000 psi. Thus, instantaneously the incremental load of -1000 psi must be carried by the squeeze film and from equation (31) $d\epsilon/dt = 9.85$ in./in./sec. The final steady-state position must correspond to the wedge film carrying the entire 2000-psi load. At that time the load number would be doubled to 166 and from Fig.21 the new eccentricity ratio will be about 0.943. If the rapidly increasing capacity of the wedge film and the slow increase in capacity of the squeeze film are ignored, the time required to move from $\epsilon = 0.93$ to $\epsilon = 0.943$ at the initial rate of 9.85 in./in./sec is only about 0.0013 sec.

Since it is impossible to apply such a load instantaneously and since the load that must be carried by the squeeze film decreases rapidly as the wedge-film capacity increases with increasing eccentricity ratio, it becomes obvious that any step-by-step procedure would have to be done in terms of time increments in the order of tenths of a millisecond and that for all practical purposes the effect of the squeeze film is inconsequential and can be neglected.

For thicker films, for example, when the incremental load acts in the opposite direction to the static load, the wedge film has relatively little capacity, it may even be negative, and the pumping action of the squeeze film will effectively help support the load until the journal approaches its new steady-state position.

SIGNIFICANCE OF L/D

The remaining major factor is the effect of the ratio of length to diameter on the performance of the squeeze film. Since only the ratio L/D = 1 has been used in tests to date, all conclusions must be inferred by comparison with the wedge-film case for which DuBois, Ocvirk, and Wehe (20) have reported experimental results for ratios of L/D from 1/4 to 2. There is no apparent reason for expecting end leakage to have an appreciably different effect on the load capacity of the squeeze film than it does on the wedge film. Therefore, until proven otherwise, it is suggested that the designer follow the recommendations of DuBois, et al, which are simply to calculate the load number by using the actual value of $(L/D)^2$ when $L/D < 1$ and to let $(L/D)^2 = 1$ when $L/D \geq 1$. For loads other than completely reversed, the load number has little meaning and the designer must work directly with the load capacity of the squeeze film. In this case the procedure would be to modify equation (25) by multiplying the right-hand side by $(L/D)^2$ to give

$$P = 4.69\,\mu\left(\frac{R}{C}\right)^2\left(\frac{L}{D}\right)^2\left(\frac{h}{C}\right)^{-.28}\left(\frac{dh/dt}{h}\right) \qquad (32)$$

and to follow the above recommendations with respect to the value of $(L/D)^2$.

[illegible]

[illegible] with zero angular motion of the load, the journal, and the bearing are:

(a) A [illegible] in trends, the actual load capacity is considerably less than predicted by existing analytical solutions.

(b) Except for very [illegible] loaded bearings, the load is supported almost entirely by positive pressures developed in the half of the bearing in which the film thickness is decreasing.

(c) The most critical factor in determining the behavior is the filling up of the space on the unloaded side of the bearing.

(d) Stefan's solution for approaching flat plates cannot be applied directly to predicting the behavior of an actual bearing.

(e) A piston with rounded ends in a cylinder is a more appropriate model than the approaching flat plates.

(f) The modification of Stefan's equation by introducing an experimentally determined area-factor k-results in an analytical expression that provides considerable insight into basic behavior characteristics, permits a reasonable prediction of behavior for sinusoidal loads, and offers a method for estimating the behavior under any type of varying load.

(g) In comparison with the wedge film, the squeeze film is relatively ineffective in supporting a load in the critical region of thin films.

ACKNOWLEDGMENTS

In addition to Messrs. Ehret, Whitlock, Brunner, and Smith, whose contributions have already been noted, the author would like to acknowledge the assistance of Mr. Richard H. Thompson, who, also as part of his fifth-year project, participated in much of the work presented here in relation to the area-factor concept.

The author would also like to express his appreciation to Prof. F.W. Ocvirk for his many valuable comments and suggestions and to the Sibley School of Mechanical Engineering at Cornell University for its financial assistance.

REFERENCES

1 J.T. Burwell, "The Calculated Performance of Dynamically Loaded Sleeve Bearings," Trans. ASME, vol. 69, 1947, pp. A-231 - A-245.

[illegible] J.T. Burwell, "The Calculated Performance of Dynamically Loaded Sleeve Bearings - II," Journal of Applied Mechanics, Trans. ASME, [illegible], pp. [illegible].

[illegible] J.T. Burwell, "The Calculated Performance of Dynamically Loaded Sleeve Bearings - III," Journal of Applied Mechanics, Trans. ASME, vol. [illegible], pp. [illegible].

[illegible] W.J. Harrison, "The Hydrodynamical Theory of the Lubrication of a Cylindrical Bearing Under Variable Load, and of a Pivot Bearing," Trans. Cambridge Philosophical Society, vol. [illegible], pp. [illegible].

5 H.W. Swift, "Fluctuating Loads in Sleeve Bearings," Journal of the Institution of Civil Engineers, vol. [illegible], 193[illegible], pp. 161-[illegible].

6 A.F. Underwood, "Rotating-Load Bearings - a New Concept of Operation and a Frictionless Support," ASME Preprint No. 44-A-29, 1944.

7 M.J. Stefan, "Versuche uber die scheinbare Adhasion," Sitzungsberichte der Mathematisch-Naturwissenschaftlichen Klasse der Kaiserlichen Akademie der Wissenschaften, vol. 69, part 2, nos. 1 to 5, 1874, pp. 713-735.

8 J.M. Stone and A.F. Underwood, "Load-Carrying Capacity of Journal Bearings," Quarterly Trans., SAE, vol. 1, Jan., 1947, pp. 56-67.

9 E.M. Simons, "The Hydrodynamic Lubrication of Cyclically Loaded Bearings," Trans. ASME, vol. 72, 1950, pp. 805-816.

10 R.W. Dayton and E.M. Simons, "Hydrodynamic Lubrication of Cyclically Loaded Bearings," Tech. Note 2544, National Advisory Committee for Aeronautics, Nov., 1951.

11 R.W. Dayton, E.M. Simons, and F.A. Fend, "Discrepancies Between Theoretical and Observed Behavior of Cyclically Loaded Bearings," Tech. Note 2545, National Advisory Committee for Aeronautics, Nov., 1951.

12 G.S.A. Shawki, "Journal-Bearing Performance for Combinations of Steady, Fundamental, and Low-Amplitude Harmonic Components of Load," Trans, ASME, vol. 78, 1956, pp. 449-455.

13 G.S.A. Shawki, "Analytical Study of Journal Bearing Performance Under Variable Loads," Trans. ASME, vol. 78, 1956, pp. 457-464.

14 G.S.A. Shawki, "Journal Bearing Performance Under Sinusoidally Alternating and Fluctuating Loads," Proc. Institution of Mechanical Engineers, vol. 169, 1955, pp. 689-698.

15 D.D. Fuller, Theory and Practice of Lubrication for Engineers, John Wiley and Sons, Inc., 1956, pp. 136-145.

16 R.M. Phelan, "The Design and Development of a Machine for the Experimental Investigation of Dynamically Loaded Sleeve Bearings," thesis, Cornell University, Ithaca, N.Y., 1950.

[illegible] W.L. Smith, "Experimental Investigation of Dynamically Loaded Sleeve Bearings with No Shaft Rotation," thesis, Cornell University, Ithaca, N.Y., [illegible].

[illegible] M.C. Shaw and E.F. Macks, Analysis and Lubrication of Bearings, McGraw-Hill Book Company, Inc., 1949.

[illegible] F.W. Ocvirk, "Short Bearing Approximation for Full Journal Bearings," Tech. Note [illegible], National Advisory Committee for Aeronautics, [illegible].

[illegible] G.B. DuBois, F.W. Ocvirk, and R.L. Wehe, "Experimental Investigations of Eccentricity Ratio, Friction, and Oil Flow of Long and Short Journal Bearings with Load-Number Charts," Tech. Note [illegible], National Advisory Committee for Aeronautics, [illegible].

[illegible] J.A. Cole and C.J. Hughes, "Oil Flow and Film Extent in Complete Journal Bearings," Proc. Institution of Mechanical Engineers, vol. [illegible], [illegible]6, pp. [illegible].

[illegible] M.N. [illegible], "The Behavior of the Lubricating Film and Side Leakage in Dynamically Loaded Bearings," Trans. ASME, vol. [illegible], [illegible], pp. [illegible].

END

FILMED

DATE: 1-95

DTIC